Vorticity reversal in curved electron waveguides

E. Šimánek
147 Oliver Road, Santa Barbara, California 93109
(Received 6 October 1998)

The switching of vorticity sign taking place in a curved electron waveguide, at the energy of the reflection resonance, is studied analytically. We consider a planar strip with a localized bend and obtain a formula for the vorticity in the transmission region. The vorticity reversal is shown to originate from the sudden change of the phase of the transmission matrix as the electron energy passes through the resonance. The alternating sign of rotation in the vortex street along the center curve of the waveguide is also explained. An exponential decay of vortex strength with the distance from the bend is predicted. [S0163-1829(99)00215-5]

I. INTRODUCTION

Vortices induced by ballistic transport past an obstacle in a quantum waveguide are the subject of increasing interest.[1–5] It was reported by Hirschfelder and Tang[1] that vortices in an L-shaped channel suddenly change the sign of rotation (chirality) as the energy passes through the reflection resonance. In a more recent study, Berggren and Ji[3] reported similar behavior of the vortex pattern induced by electron transport in a waveguide with a circular bend. The results of Refs. 1 and 3 are based on solving the Schrödinger equation by matching the wave-function amplitudes and derivatives at the boundaries separating the incident, transmission, and the corner (or bend) region. It should be interesting to have an analytic alternative to these numerical calculations so that a deeper insight into this intriguing effect is gained.

In this paper, we consider electron transport in a planar strip of fixed width containing a localized bend.[6,7] Our goal is to derive an expression for the vorticity in the transmission region. Scattering by a localized bend was considered by Goldstone and Jaffe[7] within the single channel approximation. Since wave functions containing nodal points in the strip are necessary for seeding of vortices,[1] the second transverse channel must be included in the scattering problem. The case of one propagating mode and one evanescent mode in the presence of a δ-function scatterer was studied by Bagwell.[8] We find his general approach useful for finding the transmission amplitudes in the presence of a localized bend. However, it is necessary to take into account the fact that the dependence of the scattering potential on the transverse coordinate is more complicated in our case. Actually, an explicit form of the scattering potential can be deduced by rewriting the Hamiltonian of the electron in a strip into the natural curvilinear coordinates.[6,7] The effective Schrödinger equation thus obtained contains not only the curvature-induced attractive potential but also the contribution coming from the effect of the curvature on the kinetic energy operator. It is the latter contribution which is essential for the coupling of the propagating to the evanescent mode (see Refs. 9 and 10 for related applications of this operator). Using this approach, we obtain the wave function in the transmission region as a linear combination of the propagating and the evanescent waves. Expanding the wave function in a Taylor series about the nodal points, we obtain an expression for the vorticity the magnitude of which is a topological invariant whereas its chirality depends upon the phases of the transmission matrix. This result is in agreement with the reported numerically obtained vortex patterns near the reflection resonance.[1,3]

II. THE WAVE EQUATION

Following Ref. 6, the wave equation, subject to Dirichlet boundary condition, is rewritten in natural curvilinear coordinates given by the coordinate s along the reference (guiding) curve of the waveguide, and the transverse coordinate u along the normal to this curve (see Fig. 1). Expressed in these coordinates, the Hamiltonian of an electron of mass m_e is

$$\tilde{H} = -\frac{\hbar^2}{2m_e}\left[\frac{1}{J}\frac{\partial}{\partial s}\left(\frac{1}{J}\frac{\partial}{\partial s}\right) + \frac{1}{J}\frac{\partial}{\partial u}\left(J\frac{\partial}{\partial u}\right)\right], \tag{1}$$

where $J = 1 + u\gamma(s)$ is the Jacobian of the transformation from (x,y) to (s,u), and $\gamma(s)$ is the curvature of the reference curve. It is convenient to introduce the rescaled Hamiltonian

$$\bar{H} = J^{1/2}\tilde{H}J^{-1/2} = -\frac{\hbar^2}{2m_e}\left[\frac{\partial}{\partial s}(1+u\gamma)^{-2}\frac{\partial}{\partial s} + \frac{\partial^2}{\partial u^2}\right] + V(s,u), \tag{2}$$

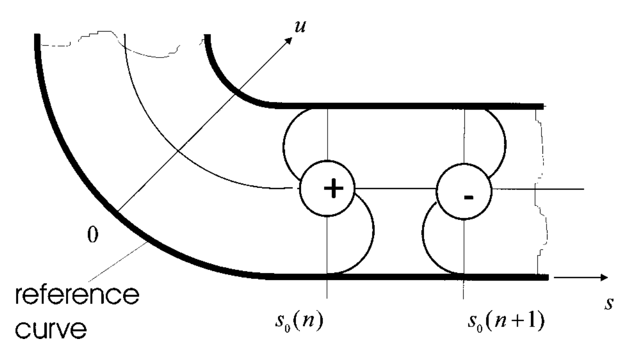

FIG. 1. Section of a curved waveguide containing vortices of opposite chirality at the adjacent nodal points in the transmission region. The curve drawn along the nodal line $s = s_0(n)$ represents the function $(-1)^n\chi_2(u)$. According to Eq. (43), this function generates the reversal of chirality as $n \rightarrow n+1$.

where $V(s,u)$ is the curvature-induced attractive potential [see Eq. (3.1b) of Ref. 6]. The corresponding rescaled wave function is given by $\phi = J^{1/2}\psi$, where ψ is the original wave function. It satisfies the Schrödinger equation

$$\bar{H}\phi(s,u) = E\phi(s,u). \tag{3}$$

The advantage of the rescaling is that ϕ is normalized on the strip.[6]

As long as the curvature radius is large compared to the width d of the strip, the Hamiltonian $\bar{H}$ can be approximated as

$$\bar{H} = \bar{H}_0 + \bar{H}_1, \tag{4}$$

where $\bar{H}_0$ is the Hamiltonian for a straight strip obtained from Eq. (1) by setting $J=1$. $\bar{H}_1$ represents the curvature-induced perturbation of the form

$$\bar{H}_1(s,u) = \frac{\hbar^2 u}{m_e}\left[\gamma(s)\frac{\partial^2}{\partial s^2} + \frac{d\gamma}{ds}\frac{\partial}{\partial s}\right] - \frac{\hbar^2\gamma(s)^2}{8m_e}. \tag{5}$$

To solve the wave equation (3), we use the ansatz[8]

$$\phi(s,u) = \sum_n c_n(s)\chi_n(u), \tag{6}$$

where $\chi_n(u)$ satisfies the Schrödinger equation for an electron moving in the transverse direction in an infinite square-well potential of width d. The corresponding energy eigenvalue is $E_n = \hbar^2\pi^2 n^2/(2m_e d^2)$. Inserting the ansatz (6) into the wave equation (2), multiplying both sides by $\chi_m^*(u)$, and integrating over u, we obtain the following coupled system of equations for the functions $c_m(s)$:

$$\frac{d^2 c_m(s)}{ds^2} + k_m^2 c_m(s) = \sum_n \Gamma_{mn}(s)c_n(s), \tag{7}$$

where

$$\Gamma_{mn}(s) = (2m_e/\hbar^2)\int_0^d \chi_m^*(u)\bar{H}_1(s,u)\chi_n(u)\,du. \tag{8}$$

The wave vector k_m is given by

$$k_m^2 = 2m_e(E - E_m)/\hbar^2. \tag{9}$$

III. TRANSMISSION AMPLITUDES

We now consider a planar strip with a bend localized at $s=0$. The bend has a characteristic length l which is of the order of the radius of the curvature.[7] The curvature $\gamma(s)$, for such a localized bend, can be approximated by a constant value $1/l$ over the interval $-l/2 < s < l/2$, and by zero outside this interval. Using this approximation in Eq. (8), we obtain

$$\Gamma_{mn}(s) = -\frac{\delta_{mn}\gamma(s)}{4l} + 2u_{mn}\left[\gamma(s)\frac{\partial^2}{\partial s^2} + \frac{d\gamma}{ds}\frac{\partial}{\partial s}\right], \tag{10}$$

where $\gamma(s)$ can be written as a difference of unit step functions,

$$\gamma(s) = [\theta(s+l/2) - \theta(s-l/2)]/l, \tag{11}$$

and

$$u_{mn} = \int_0^d \chi_m^*(u)\,u\,\chi_n(u)\,du. \tag{12}$$

In the limit $l\to 0$, the function $\gamma(s)$ goes over to a δ function. We note that this limiting process allows us to reduce the solution of Eqs. (7) to a system of algebraic equations.[8] The idea is to integrate Eq. (7) over the interval $-l/2 < s < l/2$, and subsequently let $l\to 0$. In this way, we obtain with the use of Eq. (11)

$$\left.\frac{dc_m(s)}{ds}\right|_{s=0^+} - \left.\frac{dc_m(s)}{ds}\right|_{s=0^-} = \sum_n I_{mn}, \tag{13}$$

where

$$I_{mn} = -\frac{\delta_{mn}c_n(0)}{4l} + \frac{2u_{mn}}{l}\left[\left.\frac{dc_n}{ds}\right|_{s=0^+} - \left.\frac{dc_n}{ds}\right|_{s=0^-}\right]. \tag{14}$$

Equations (13) are to be solved with the boundary condition ensuring the continuity of the wave function at $s=0$,

$$c_m(s=0^+) = c_m(s=0^-). \tag{15}$$

A remark concerning the validity of the limit $l\to 0$ for the bent waveguide is in order. If the wave function varies slowly over the interval $-l/2 < s < l/2$, the limiting process leading to Eq. (13)–(15) is valid. In what follows, we consider a propagating mode with the energy $E \approx E_2$. The corresponding wave vector k_1 is, according to Eq. (9), of the order of $1/d$. In deriving Eqs. (4) and (5), we assumed that the length of the bend exceeds the width of the strip, which implies $k_1 l \gg 1$ and the limiting process is not valid. The finite length of the potential well [the last term of Eq. (5)] is responsible for transmission resonances which are washed out in the limit $l\to 0$. Since our main concern is the transmission zero, this error is of no qualitative consequence. As for the evanescent mode, the corresponding wave vector $\kappa_2 \gg k_1$ so that the limiting process is acceptable.

For propagating modes incident on the left of the bend, the amplitude $c_m(s)$ is, for $s<0$, a superposition of the incident and reflected waves

$$c_m(s) = A_m e^{ik_m s} + B_m e^{-ik_m s}. \tag{16}$$

For $s>0$, we have a transmitted wave

$$c_m(s) = C_m e^{ik_m s}. \tag{17}$$

The boundary condition (15) implies

$$A_m + B_m = C_m. \tag{18}$$

The evanescent mode is obtained from Eq. (16) by setting $k_m = i\kappa_m$, and $A_m = 0$. Taking into account condition (18), we have for all values of s

$$c_m(s) = C_m e^{-\kappa_m|s|}, \tag{19}$$

where

$$\kappa_m^2 = 2m_e(E_m - E)/\hbar^2. \tag{20}$$

For one propagating and one evanescent mode with wave vectors k_1 and $i\kappa_2$, respectively, the coupled equations (13) become, with the use of Eqs. (14)–(19),

$$(2ik_1+1/l)C_1+4(u_{12}/l)\kappa_2 C_2=2ik_1 A_1,$$

$$4ik_1(u_{12}/l)C_1+(2\kappa_2-1/l)C_2=4ik_1(u_{12}/l)A_1. \quad (21)$$

Defining the transmission amplitudes $t_{11}=C_1/A_1$ and $t_{12}=C_2/A_1$, Eqs. (21) yield

$$t_{11}=\frac{-2ik_1+16ik_1\kappa_2(u_{12}/l)^2/(2\kappa_2-1/l)}{-2ik_1-1/l+16ik_1\kappa_2(u_{12}/l)^2/(2\kappa_2-1/l)},$$

$$t_{12}=\frac{4ik_1(u_{12}/l)(1-t_{11})}{2\kappa_2-1/l}. \quad (22)$$

According to Eq. (22), the numerator of t_{11} vanishes when

$$\kappa_2[1-4(u_{12}/l)^2]=1/(2l). \quad (23)$$

Using Eq. (20), we obtain from Eq. (23) the energy at which $t_{11}=0$. This is the quasi-bound-state energy

$$E_b=E_2-\frac{\hbar^2}{8m_e l^2 r^2}, \quad (24)$$

where

$$r=1-4(u_{12}/l)^2. \quad (25)$$

Of particular importance for the study of vorticity in the neighborhood of E_b turns out to be the phase λ_1 defined by

$$t_{11}=|t_{11}|e^{i\lambda_1}. \quad (26)$$

From Eq. (22) we find, expanding about E_b,

$$\lambda_1=\tan^{-1}\left[\frac{\Gamma}{E_b-E}\right], \quad (27)$$

where

$$\Gamma=\frac{\hbar^2 d u_{12}^2}{2\sqrt{3}m_e l^5 r^3}. \quad (28)$$

Since Γ is positive, we see from Eq. (27) that λ_1 changes suddenly from $\pi/2$ to $-\pi/2$ as the energy passes through E_b from below. We note that an expression similar to Eq. (27) also describes the phase shift at the transmission resonance.[11] This is in accord with the fact that a change of phase shift by π is generally expected at resonance scattering.[12]

From Eq. (22), we see that t_{12} has a pole at the energy

$$E_0=E_2-\frac{\hbar^2}{8m_e l^2}. \quad (29)$$

On comparing this result with Eq. (24), we see that $E_0>E_b$, the difference being

$$E_0-E_b\approx\frac{\hbar^2 u_{12}^2}{m_e l^4}, \quad (30)$$

where we assumed $u_{12}/l\ll 1$. There is no sudden change of the phase of t_{12}, λ_2, as the energy passes through E_b.

IV. VORTICITY

We focus on the transmission region, $s>0$, where the wave function is, according to Eqs. (6), (17), and (19),

$$\phi(s,u)=L^{-1/2}[t_{11}e^{ik_1 s}\chi_1(u)+t_{12}e^{-\kappa_2 s}\chi_2(u)], \quad (31)$$

where L is the length of the strip in the s direction, and

$$\chi_1(u)=\left(\frac{2}{d}\right)^{1/2}\sin\frac{\pi u}{d},$$

$$\chi_2(u)=\left(\frac{2}{d}\right)^{1/2}\sin\frac{2\pi u}{d}. \quad (32)$$

The position of the nodes, (s_0,u_0), of the wave function is obtained by setting both the real and the imaginary parts of Eq. (31) equal to zero. In this way, we obtain

$$s_0(n)=k_1^{-1}(\lambda_2-\lambda_1+n\pi) \quad (33)$$

and

$$\frac{\pi u_0}{d}=2\pi m+\cos^{-1}\left[\frac{(-1)^{n+1}|t_{11}|e^{\kappa_2 s_0}}{2|t_{12}|}\right], \quad (34)$$

where n in Eq. (33) and m in Eq. (34) are any positive or negative integers.[1] When the energy E is close to the reflection resonance, Eq. (9) yields $k_1\approx\sqrt{3}\pi/d$. Using this result in Eq. (33), we see that the nodal points (vortex centers) are spaced equally by $d/\sqrt{3}$ along the s direction. In the neighborhood of the transmission zero ($|t_{11}|=0$), Eq. (34) shows that $u_0\approx d/2$ (see Fig. 1). This implies that the vortex street runs close to the center curve of the waveguide. The streamlines reported in Refs. 1 and 3 are in agreement with these predictions.

Expanding the wave function (31) about the nodal point, (s_0,u_0), to first order, we have

$$\phi(s,u)\simeq a(u-u_0)+ib(s-s_0), \quad (35)$$

where

$$a=\left(\frac{2}{Ld}\right)^{1/2}\left[t_{11}\cos\frac{\pi u_0}{d}e^{ik_1 s_0}+2t_{12}\cos\frac{2\pi u_0}{d}e^{-\kappa_2 s_0}\right]\frac{\pi}{d},$$

$$b=\left(\frac{2}{Ld}\right)^{1/2}\left[k_1 t_{11}\sin\frac{\pi u_0}{d}e^{ik_1 s_0}+i\kappa_2 t_{12}\sin\frac{2\pi u_0}{d}e^{-\kappa_2 s_0}\right]. \quad (36)$$

The vorticity q is defined as a circulation of the velocity $\mathbf{v}$,

$$q=(2\pi)^{-1}\oint_{(C)}\mathbf{v}\cdot d\mathbf{s}, \quad (37)$$

where C is a closed curve surrounding the nodal point.[1,5]

Expressing the wave function (35) in the form

$$\phi(s,u)=|\phi(s,u)|e^{i\theta(s,u)} \quad (38)$$

the velocity $\mathbf{v}$ becomes

$$\mathbf{v}=\frac{\hbar}{m_e}\boldsymbol{\nabla}\theta=\frac{\hbar}{m_e}\boldsymbol{\nabla}\left[\tan^{-1}\frac{a_2(u-u_0)+b_1(s-s_0)}{a_1(u-u_0)-b_2(s-s_0)}\right], \tag{39}$$

where subscripts 1 and 2 indicate the real and the imaginary parts, respectively. Inserting this result into Eq. (37), and performing the integration with C being a circle centered at the nodal point, we obtain (see Sec. 1 of the Appendix)

$$q=\frac{\hbar(ab^*+a^*b)}{m_e|ab^*+a^*b|}. \tag{40}$$

Using Eqs. (33), (34), and (36), we obtain

$$ab^*+a^*b=\frac{8\pi k_1}{Ld^2}(-1)^{n+1}|t_{11}||t_{12}|e^{-\kappa_2 s_0}\sin\frac{\pi u_0}{d}. \tag{41}$$

From this result we see that the sign of the vorticity q in Eq. (40) is determined by the factor $(-1)^{n+1}$. Thus, we obtain

$$q=\frac{\hbar}{m_e}(-1)^{n+1}. \tag{42}$$

To apply the present theory to the vortex patterns observed in Refs. 1 and 3, we need to consider Eq. (42) in conjunction with Eq. (33). Let us first consider the case of a fixed energy $E\approx E_b$. Then the quantities k_1, λ_1, and λ_2 are fixed and Eq. (33) describes a series of equidistant vortices spaced along the s coordinate by a distance π/k_1. A shift of s_0 by this spacing amounts to a change of the integer n by 1 (see Fig. 1). Equation (42) implies that a change of the sign of the vorticity is associated with this shift. This explains the alternation of the rotation sign of the vortices reported in Refs. 1 and 3.

Next, we focus on a given site s_0 and ask about the changes of the vorticity as the energy E passes through the reflection resonance. According to Eq. (27), the quantity λ_1 changes suddenly by $-\pi$ as E moves through E_b from below. Since λ_2 does not change, and s_0 is fixed, we see from Eq. (33) that a change of $n\rightarrow n-1$ takes place. With the use of Eq. (42), a change of the vorticity sign is obtained at the site s_0 in agreement with the numerical results.[1,3]

V. CURRENTS AND VORTEX STRENGTH

A somewhat less formal way of understanding these effects is to consider, instead of **v**, the probability current density **J**. This quantity has the same properties as far as the vortex chirality is concerned. Moreover, it determines the vortex strength, for example, through the vortex-induced magnetic moment.[5] To illustrate the mechanism of chirality switching, we consider the component J_s at a fixed position s_0 as a function of u. Assuming that s_0 lies in the straight section of the waveguide $(\gamma=0)$, and using Eq. (31), we have

$$\begin{aligned}J_s(s_0,u)&=\frac{i\hbar}{2m_e}\left(\phi\frac{\partial\phi^*}{\partial s}-\text{c.c.}\right)\bigg|_{s=0}\\&=\frac{\hbar k_1}{m_eL}[|t_{11}|^2\chi_1^2(u)\\&\quad+(-1)^n e^{-\kappa_2 s_0}|t_{11}||t_{12}|\chi_1(u)\chi_2(u)].\end{aligned} \tag{43}$$

The first term on the right-hand side of Eq. (43) represents the current transmitted in the first transverse mode. Since it is symmetric about the center curve, $u=d/2$, it does not contribute to the vorticity of a vortex located at s_0, $u_0\approx d/2$. The second term is due to the mixing of the propagating and the evanescent mode. Its dependence upon u is controlled by the product $\chi_1(u)\chi_2(u)$. This product is an odd function of u about the center point $u_0=d/2$. Hence, it contributes to the vorticity. As the integer n changes by one, this product switches sign (see Fig. 1). According to Eq. (33), this can be achieved by shifting $s_0(n)$ to $s_0(n\pm1)$, or by changing the phase λ_1 by $\pm\pi$. Expanding Eq. (43) about $u=u_0$, to first order, we find

$$J_s=\frac{\hbar}{2m_e}(ab^*+a^*b)(u-u_0). \tag{44}$$

In a similar way, we find

$$J_u=-\frac{\hbar}{2m_e}(ab^*+a^*b)(s-s_0). \tag{45}$$

We see that it is the same factor, ab^*+a^*b, which determines both the vorticity [see Eq. (40)] and the local current density near the vortex center. The latter can be used to estimate the vortex strength Γ, defined as the circulation of the probability current density,

$$\Gamma=\oint_{(C)}\mathbf{J}\cdot d\mathbf{s}=-\frac{\hbar A}{m_e}(ab^*+a^*b), \tag{46}$$

where we used Eqs. (44) and (45). Here A stands for the area enclosed by the contour C. The dependence of Eq. (46) on A is contrary to the expectation that the vortex strength is a topologically invariant quantity. The problem is that the first-order expansions about the nodal point, used in Eqs. (44) and (45), do not correctly describe the asymptotic long-range behavior of the current. Rather, they are appropriate for the inner region $r\ll\xi$, where r is the distance from the nodal point and ξ is the characteristic length. We can determine this length by proceeding in analogy with the nonlinear Schrödinger equation.[13] We note that the nonlinearity does not influence the characteristic length scale of this equation, rather it determines the normalization of the wave function. Applying this analogy to Eq. (3), we see that the characteristic scale at which the expansions (44) and (45) break down is given by

$$\xi=\left[\frac{\hbar^2}{2m_eE}\right]^{1/2}. \tag{47}$$

Since $E\approx E_2$, we obtain from Eq. (43) $\xi\approx d/(2\pi)$. We can identify this distance with the approximate size of the vortex core. It follows that Eq. (46) holds only if the integration contour C lies within the core region. Outside the core region, the expansion of **J** must be carried out beyond the first order. In fact, if we were to calculate the induced magnetization density, the current density should be calculated from the full expression (31).

Nevertheless, some qualitative conclusions can be drawn from Eq. (46). From the proportionality of Γ to ab^*+a^*b, we see that the vortex strength exhibits not only the chirality switching [factor $(-1)^n$], but also an exponential decay represented by the factor $e^{-k_2 s_0}$. The streamlines shown in Refs. 1 and 3 do not extend sufficiently far into the transmission region to show this decay of vortex strength.

The calculation of the vorticity, shown in Sec. 1 of the Appendix, is also based on the first-order expansion (35). Strictly speaking, this imposes a restriction on the radius of the circle, chosen for the integration contour in Eq. (A1). However, this radius cancels out on going to Eq. (A2), yielding a topologically invariant result. This is related to the definition, Eq. (39), of the velocity in terms of $\nabla\theta$. The vorticity (37) is thus proportional to the circulation of $\nabla\theta$ which is equal to $\pm 2\pi$. Hence, our conclusions about vortex chirality are not affected by the approximation (35).

VI. SUMMARY

A simple model of an electron waveguide containing a localized bend is used to study, analytically, the vorticity in the transmission region. The coupling of the propagating and the evanescent modes by the curvature-induced perturbation is found essential for the formation of vortices. For energies near the reflection resonance, the vortices form a street running close to the center of the waveguide. An expression for the vorticity is derived which explains the alternation of chirality along the street, and the overall reversal of the vorticity as the energy passes through the reflection resonance (effects previously seen in numerical studies).[1,3] The sudden change of the phase of the transmission amplitude at the resonance is found responsible for this effect. Associated with this is the change of the sign of the admixture of the evanescent mode. Calculation of the current density along the nodal lines as a function of the transverse coordinate confirms that this sign change produces a reversal of the current circulating about the nodal point. The vortex strength, obtained with this current density, exhibits an exponential decay with the distance from the bend.

ACKNOWLEDGMENTS

I thank Pavel Exner and Lawrence Schulman for inspiring correspondence.

APPENDIX

1. Derivation of Eq. (40)

For nodal points situated in the straight transmission region, the evaluation of the velocity circulation is simplified by setting $\gamma=0$. Consequently, we replace the curvilinear coordinates in Eq. (39) by rectangular ones: $(s-s_0)\to x$ and $(u-u_0)\to y$. Using Eq. (39) in Eq. (37), we obtain

$$q=\frac{\hbar(ab^*+a^*b)}{4\pi m_e}\oint_{(C)}\frac{x\,dy-y\,dx}{|ay+ibx|^2}. \tag{A1}$$

Assuming that C is a circle centered at $x=0$, $y=0$, and going over to polar coordinates, (r,α), Eq. (A1) becomes

$$q=\frac{\hbar(ab^*+a^*b)}{4\pi m_e}\int_0^{2\pi}\frac{d\alpha}{|a\sin\alpha+ib\cos\alpha|^2}. \tag{A2}$$

The angular integral is evaluated in the complex z plane. We set $z=e^{i\alpha}$, and obtain from Eq. (A2)

$$q=\frac{i\hbar}{\pi m_e(a-b)(a^*+b^*)}\times\oint_{|z|=1}\frac{z\,dz}{(z-z_1)(z-z_2)(z-z_3)(z-z_4)}, \tag{A3}$$

where

$$z_{1,2}=\pm\left(\frac{a+b}{a-b}\right)^{1/2},$$

$$z_{3,4}=(z_{1,2}^*)^{-1}. \tag{A4}$$

Only the pole which lies within the unit disk in the z plane contributes to the integral (A3). From Eq. (A4), we have

$$|z_{1,2}^2|^2=\frac{|a|^2+|b|^2+(a^*b+ab^*)}{|a|^2+|b|^2-(a^*b+ab^*)}. \tag{A5}$$

We see that the poles $z_{1,2}$ contribute only if $a^*b+ab^*<0$. In this case, the poles $z_{3,4}$ lie outside the unit disk, and formula (A3) yields $q=-\hbar/m_e$.

On the other hand, if $a^*b+ab^*>0$, only the poles $z_{3,4}$ contribute, yielding $q=\hbar/m_e$.

2. Derivation of Eq. (41)

With the use of Eq. (36), we obtain

$$ab^*+a^*b=\frac{2\pi k_1}{Ld^2}\left[|t_{11}|^2\sin\frac{2\pi u_0}{d}+2\cos\frac{2\pi u_0}{d}\sin\frac{\pi u_0}{d}e^{-\kappa_2 s_0}\times(t_{12}t_{11}^*e^{ik_1 s_0}+\text{c.c.})\right]. \tag{A6}$$

We note that cross terms, proportional to κ_2, cancel out owing to the identity [obtained with the use of Eq. (33)]

$$t_{12}t_{11}^*e^{ik_1 s_0}=|t_{11}||t_{12}|(-1)^n. \tag{A7}$$

Using this identity in the second term of Eq. (A6), we have

$$ab^*+a^*b=\frac{4\pi k_1}{Ld^2}\sin\frac{\pi u_0}{d}\left[|t_{11}|^2\cos\frac{\pi u_0}{d}+2|t_{11}||t_{12}|e^{-\kappa_2 s_0}(-1)^n\cos\frac{2\pi u_0}{d}\right]. \tag{A8}$$

From Eq. (34), we obtain

$$\cos\frac{\pi u_0}{d}=(-1)^n\frac{|t_{11}|e^{\kappa_2 s_0}}{2|t_{12}|} \tag{A9}$$

and

$$\cos\frac{2\pi u_0}{d}=\frac{|t_{11}|^2e^{2\kappa_2 s_0}}{2|t_{12}|^2}-1. \tag{A10}$$

Inserting Eqs. (A9) and (A10) into Eq. (A8) and noting cancellation of the terms proportional to $e^{\kappa_2 s_0}$, we arrive at Eq. (41).

[1] J. O. Hirschfelder and K. T. Tang, J. Chem. Phys. **64**, 760 (1976).
[2] C. S. Lent, Appl. Phys. Lett. **57**, 1678 (1990).
[3] K. F. Berggren and Zhen-Li Ji, Phys. Rev. B **47**, 6390 (1993).
[4] Hua Wu and D. W. L. Sprung, Phys. Lett. A **183**, 413 (1993).
[5] P. Exner, P. Šeba, A. F. Sadreev, P. Středa, and P. Feher, Phys. Rev. Lett. **80**, 1710 (1998).
[6] P. Exner and P. Šeba, J. Math. Phys. **30**, 2574 (1989).
[7] J. Goldstone and R. L. Jaffe, Phys. Rev. B **45**, 14 100 (1992).
[8] P. F. Bagwell, Phys. Rev. B **41**, 10 354 (1990).
[9] J. Marcus, J. Chem. Phys. **45**, 4493 (1966).
[10] E. Šimánek, Phys. Rev. B **57**, 14 634 (1998).
[11] G. Baym, *Lectures on Quantum Mechanics* (Benjamin, New York, 1969).
[12] J. R. Taylor, *Scattering Theory* (Wiley, New York, 1972).
[13] V. L. Ginzburg and L. P. Pitaevskii, Zh. Eksp. Teor. Fiz. **34**, 1240 (1958) [Sov. Phys. JETP **7**, 858 (1958)].